Elastoplastic Model for Transversely Isotropic Rocks

Zhechao Wang[1]; Zhi Zong[2]; Liping Qiao[3]; and Wei Li[4]

Abstract: The structure of the layered rocks is characterized by oriented bedding planes, resulting in transverse isotropy in deformation and strength. An elastoplastic constitutive model was proposed for transversely isotropic (TI) rock in this study. In the model, the generalized Hooke's law was adopted for the elastic behavior. For the plastic behavior, the yield criterion and plastic potential are formulated as functions of the generalized octahedral shear stress and the first invariant of stress tensor. A nonassociated flow rule and a stress-dependent hardening rule were adopted in the model. The plastic model can be simplified to the Drucker-Prager model for isotropic rocks. A methodology for the determination of model parameters was developed. The parameters can be determined by combining triaxial compression tests with torsion tests on specimens with different bedding directions. The constraint on plastic parameters was theoretically identified. The proposed model and the parameter determination methodology were applied to modeling the TI elastoplastic property of carbonaceous slate in triaxial compression. The results show that the model proposed in this study can well describe the transverse isotropic elastoplastic property of the rock, and the parameter determination methodology is simple and effective. **DOI: 10.1061/(ASCE)GM.1943-5622.0001070.**

Author keywords: Rock; Transversely isotropic (TI); Elastoplastic property; Constitutive modeling; Parameter determination; Plastic flow.

Introduction

Anisotropic rocks are common on earth. Both metamorphic and sedimentary rocks have inherent or structural anisotropy (Barton and Quadros 2015). Among them, layered rocks are usually encountered in tunneling, geoenergy exploration, CO_2 underground disposal, and underground space development. The structure of the layered rocks is characterized by oriented bedding planes or foliations, resulting in transverse isotropy in deformation and strength of the rocks. Because they have similar properties within the bedding planes, the layered rock masses can be treated as transversely isotropic (TI) material. The experimental data show that the elastic modulus in the bedding plane is approximately 1.5 times that in the direction perpendicular to the bedding plane for many layered rocks (Amadei 1996). The deformation and strength differ several times when the rocks are subjected to different loading directions (Amadei 1996; Tien et al. 2006; Gao et al. 2011; Liu et al. 2013; Shi et al. 2016). Because of the directional nature of layered rocks, the determination of mechanical parameters and in situ stress fields, and the estimation on the bearing capacity of rock foundation and deformation of surrounding rocks around tunnels using the isotropic model will cause significant deviations from the actual situations (Amadei 1996; Hefny and Lo 1999; Ding et al. 2006; Hakala et al. 2007; Bobet 2011; Zhang and Sun 2011; Vu et al. 2013b; Simanjuntak et al. 2016). Nevertheless, the TI constitutive models for rocks have more parameters than the isotropic models, which make the determination of parameters for TI constitutive models worthy of investigation. Therefore, it is of great theoretical and practical value to propose an elastoplastic model for TI rocks and develop a methodology for model parameter determination.

Many models have been proposed to describe elastoplastic stress-strain responses of soils or granular materials (Nixon and Chandler 1999; Tsutsumi and Hashiguchi 2005; Anandarajah 2008; Lai et al. 2009; Muraleetharan et al. 2009; Yin et al. 2009; Kamrin 2010; Yin et al. 2010; Zhu et al. 2010; Wang and Wong 2016, 2017) and rocks (Huang and Khan 1991; Khan et al. 1991, 1992; Shao and Henry 1991; Vorobiev 2008; Chang et al. 2015; Shen and Shao 2016). Generally, a single model was developed for a specific modeling purpose. There is no one suitable way of describing all aspects of the elastoplastic behavior of the materials. On the TI elastic behavior of rocks, many research studies focused on the determination of elastic parameters (Talesnick et al. 1995; Exadaktylos 2001; Gautam and Wong 2006; Chou and Chen 2008; Liu et al. 2013). There was some literature in which theoretical solutions of the stress and the displacement fields were derived in TI rocks around an underground opening (Hefny and Lo 1999; Bobet 2011; Zhang and Sun 2011; Vu et al. 2013a; Simanjuntak et al. 2016). Compared with the studies on TI elastic property, the investigations on the TI plastic property of rocks are limited. Xu et al. (2010) addressed the TI plastic property by varying the parameters in a Drucker-Prager (DP) model with loading direction. Long et al. (2013) proposed a TI plastic model for fiber-reinforced composites in strain space. Wang et al. (2014) used the DP model to describe the plastic properties of both bedding planes in the local coordinate system and intact rock in the global coordinate system to describe the dependency of strength of the TI rocks on loading direction in relation to bedding planes. Singh et al. (2015) extended the strength criterion of an isotropic rock material based on the critical state and proposed the anisotropic nonlinear strength criterion.

Previous studies primarily focused on the TI elastic property and the strength of rocks, whereas few focused on the TI yielding and the plastic flow of rocks. The TI plastic models proposed in previous studies

[1]Professor, Key Laboratory of Ministry of Education on Safe Mining of Deep Metal Mines, Northeastern Univ., 3-11, Wenhua Rd., Shenyang, Liaoning 110819, China; Visiting Professor, State Key Laboratory of Geomechanics and Geotechnical Engineering, Institute of Rock and Soil Mechanics, Chinese Academy of Sciences, Wuhan, Hubei 430071, China (corresponding author). E-mail: wang_zhechao@hotmail.com

[2]M.Sc. Student, Shandong Univ., 17923, Jingshi Rd., Jinan, Shandong 250061, China. E-mail: 583331473@qq.com

[3]Associate Professor, Dept. of Civil Engineering, Northeastern Univ., 3-11, Wenhua Rd., Shenyang, Liaoning 110819, China. E-mail: qiaolp@mail.neu.edu.cn

[4]M.Sc. Student, Shandong Univ., 17923, Jingshi Rd., Jinan, Shandong 250061, China. E-mail: 1669605363@qq.com

Note. This manuscript was submitted on February 1, 2017; approved on September 6, 2017; published online on December 6, 2017. Discussion period open until May 6, 2018; separate discussions must be submitted for individual papers. This paper is part of the ***International Journal of Geomechanics***, © ASCE, ISSN 1532-3641.

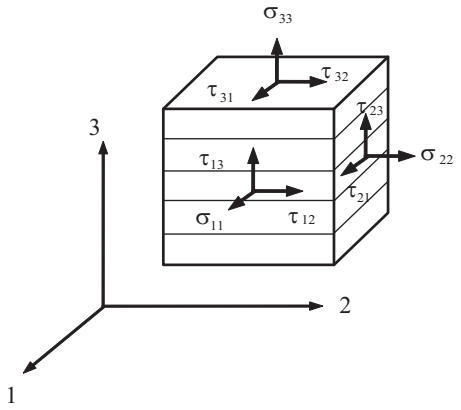

Fig. 1. Stress tensor components acting on an element of transversely isotropic material: σ_{11} and σ_{22} in isotropic planes 1 and 2, and σ_{33} in the direction perpendicular to the plane

separated the formulations for bedding planes and intact rock, which make their applications limited to the simple stressing conditions under which the formulations were derived. Because the number of parameters for TI elastoplastic models is greater than those for isotropic models, parameter determination is one of the important issues for TI plastic models. Therefore, it is necessary to perform a study aimed at proposing a generalized plastic TI model with a reasonable number of parameter and developing methods for the parameter determination.

In this study, such a generalized TI plastic model was proposed, in which the yield criterion and plastic potential are formulated as functions of the generalized octahedral shear stress and the first invariant of stress tensor. A nonassociated flow rule and a stress-dependent hardening criterion were adopted in the model. The generalized TI plastic model can be simplified to the DP model for isotropic rocks. For the sake of a complete TI elastoplasticity framework and the interaction between elastic and plastic behavior, the TI elastic model from the generalized Hooke's law also was presented in this study. A methodology for the determination of parameters for the TI elastoplastic model was developed. The proposed model and parameter determination methodology were applied to modeling the TI elastoplastic property of carbonaceous slate in triaxial compression. The results show that the model proposed in this study can well describe the TI elastoplastic property of the rock, and the parameter determination methodology is simple and effective. Several other issues, including the plastic flow directions, the interaction between elastic and plastic parameters, and the dependency of strength on the loading direction, were discussed in the light of the model.

TI Elastoplastic Model

Elasticity

The TI elastic behavior could be described using the generalized Hooke's law, in which the strain increment is a linear function of the stress increment. Assuming that the material property in the bedding planes in which both σ_{11} and σ_{22} are acting is isotropic, as shown in Fig. 1, the TI elasticity could be expressed in Eq. (1)

$$\begin{bmatrix} \Delta\varepsilon^e_{11} \\ \Delta\varepsilon^e_{22} \\ \Delta\varepsilon^e_{33} \\ \Delta\gamma^e_{23} \\ \Delta\gamma^e_{31} \\ \Delta\gamma^e_{12} \end{bmatrix} = \begin{bmatrix} \frac{1}{E_h} & -\frac{\nu_{hh}}{E_h} & -\frac{\nu_{vh}}{E_v} & 0 & 0 & 0 \\ -\frac{\nu_{hh}}{E_h} & \frac{1}{E_h} & -\frac{\nu_{vh}}{E_v} & 0 & 0 & 0 \\ -\frac{\nu_{vh}}{E_v} & -\frac{\nu_{vh}}{E_v} & \frac{1}{E_v} & 0 & 0 & 0 \\ 0 & 0 & 0 & \frac{1}{G_{vh}} & 0 & 0 \\ 0 & 0 & 0 & 0 & \frac{1}{G_{vh}} & 0 \\ 0 & 0 & 0 & 0 & 0 & \frac{2(1+\nu_{hh})}{E_h} \end{bmatrix} \times \begin{bmatrix} \Delta\sigma_{11} \\ \Delta\sigma_{22} \\ \Delta\sigma_{33} \\ \Delta\tau_{23} \\ \Delta\tau_{31} \\ \Delta\tau_{12} \end{bmatrix} \quad (1)$$

where E_v = elastic modulus perpendicular to the bedding planes; E_h = elastic modulus in the bedding planes; ν_{vh} = Poisson's ratio defined as the ratio of the strain in the isotropic plane over that in the direction perpendicular to the isotropic plane; G_{vh} = shear modulus perpendicular to the bedding planes; $\Delta\sigma_{11}$, $\Delta\sigma_{22}$, $\Delta\sigma_{33}$, $\Delta\tau_{23}$, $\Delta\tau_{31}$ $\Delta\tau_{12}$ = increments in stress tensor components in a local coordinate system; and $\Delta\varepsilon^e_{11}$, $\Delta\varepsilon^e_{22}$, $\Delta\varepsilon^e_{33}$, $\Delta\gamma^e_{23}$, $\Delta\varepsilon^e_{31}$ $\Delta\varepsilon^e_{12}$ = increments in elastic strain tensor components in a local coordinate system.

Plasticity

A plastic model consists of three parts: yield criterion, flow rule, and hardening rule. The yield criterion is used to determine the stress condition when plastic deformation starts to occur in material, the flow rule is used to describe the plastic flow direction, and the hardening rule determines the increment of plastic strain caused by the increment of stress. Well-accepted plastic models for geomaterials include the Mohr-Coulomb model, the DP Prager model, the Cam-clay model, the Lade-Duncan model, the Hoek-Brown model, and the Matsuoka-Nakai model, among others. These models describe the plastic property of geomaterials using a few parameters with clear physical meaning. However, they are incapable or limited capable of describing the TI plasticity of geomaterials.

In the study of the plasticity of metals, Hill (1950) extended the Mises model to an anisotropic plastic model for metals. In Hill's model, the yield criterion was formulated as a function of generalized octahedral shear stress. The yield function was expressed in Eq. (2) (Hill 1950)

$$g(\sigma) = \sqrt{F(\sigma_{yy}-\sigma_{zz})^2 + G(\sigma_{zz}-\sigma_{xx})^2 + H(\sigma_{xx}-\sigma_{yy})^2 + 2L\tau_{yz}^2 + 2M\tau_{zx}^2 + 2N\tau_{xy}^2} - D \quad (2)$$

where σ_{xx}, σ_{yy}, σ_{zz}, τ_{yz}, τ_{zx}, and τ_{xy} = stress tensor components in a global coordinate system; and D, F, G, H, L, M, and N = model parameters. If the model parameters are identical to unity, Hill's model will be reduced to the Mises model.

Yield Criterion

As is well documented, the yield of geomaterials is dependent on not only the shear stress but also the confining pressure or mean stress. Therefore, to describe the yield of anisotropic geomaterials, Hill's yield criterion is extended to Eq. (3)

$$g(\sigma) = \sqrt{F(\sigma_{yy} - \sigma_{zz})^2 + G(\sigma_{zz} - \sigma_{xx})^2 + H(\sigma_{xx} - \sigma_{yy})^2 + 2L\tau_{yz}^2 + 2M\tau_{zx}^2 + 2N\tau_{xy}^2} - \beta \mathrm{I}_1 - D \tag{3}$$

where I_1 = first invariant of the stress tensor; and β and D = model parameters dependent on friction angle and cohesion at yielding. Also, parameters L, M, and N are dependent on F, G, and H.

For TI rocks, assuming that the plane in which both σ_{11} and σ_{22} are acting is an isotropic plane, Eq. (3) can be simplified as Eq. (4)

$$g(\sigma) = \sqrt{F(\sigma_{22} - \sigma_{33})^2 + F(\sigma_{33} - \sigma_{11})^2 + H(\sigma_{11} - \sigma_{22})^2 + 2L\tau_{23}^2 + 2L\tau_{31}^2 + 2N\tau_{12}^2} - \beta \mathrm{I}_1 - D \tag{4}$$

The yield surface of the model is a convex angle cone surface with a nonequal intercept elliptic section. Figs. 2(a and b) show the yield lines of the yield surface in the meridian plane and π plane in the σ_{11}-σ_{22}-σ_{33} space, respectively, along with those for the DP and Hill models. The extended Hill's model is capable of describing the dependency of yield on both loading direction and confining pressure. When $F = H = 1$ and $L = N = 0$, the extend Hill's model is reduced into the DP model.

Specifically, in the triaxial compression test, all shear stress components turn to zero, and the expression of the model becomes Eq. (5)

$$g(\sigma) = \sqrt{F(\sigma_{22} - \sigma_{33})^2 + F(\sigma_{33} - \sigma_{11})^2 + H(\sigma_{11} - \sigma_{22})^2} - \beta \mathrm{I}_1 - D \tag{5}$$

In the torsion test of a horizontal bedding specimen, all normal stress components and the shear stress components τ_{23} and τ_{31} turn to zero, and the model turns to the expression

$$g(\sigma) = \sqrt{2N\tau_{12}^2} - \beta \mathrm{I}_1 - D \tag{6}$$

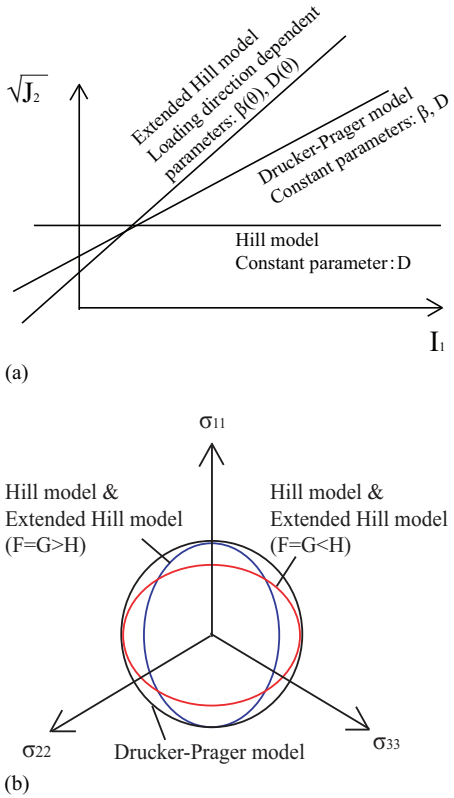

Fig. 2. Yield lines of the yield surfaces in the meridian plane (a) and π plane in the σ_{11}-σ_{22}-σ_{33} space and (b) for DP, Hill, and extended Hill models

Flow Rule

The flow rule is used to describe the plastic flow direction. Generally

$$\mathrm{d}\varepsilon_{ij}^{p} = \mathrm{d}\lambda \frac{\partial f(\sigma)}{\partial \sigma_{ij}} \tag{7}$$

where $\mathrm{d}\lambda$ = plastic factor; and f = potential function. If f is identical to g, then the flow rule is associated; if f is not identical to g, then the flow rule is nonassociated. Generally, f is not identical to g for geomaterials (Zheng and Kong 2010). Therefore, the potential function can be expressed as Eq. (8)

$$f(\sigma) = \sqrt{F(\sigma_{22} - \sigma_{33})^2 + F(\sigma_{33} - \sigma_{11})^2 + H(\sigma_{11} - \sigma_{22})^2 + 2L\tau_{23}^2 + 2L\tau_{31}^2 + 2N\tau_{12}^2} - \alpha \mathrm{I}_1 \quad (8)$$

where α = model parameter related to dilation angle and is expressed as (SIMULIA 2006)

$$\alpha = \frac{\sin\varphi}{\sqrt{3}\sqrt{3 + \sin^2\varphi}} \quad (9)$$

where φ = dilation angle. For the associated plastic flow $\alpha = \beta$, and for the nonassociated plastic flow, $\alpha \neq \beta$.

Hardening Rule

The hardening rule determines the increment of plastic strain caused by the increment of stress. Usually volumetric plastic strain is related to mean stress for volumetric hardening, and shear plastic strain is related to deviatoric stress for shear hardening. In this study, the volumetric hardening was adopted.

It should be noted that the proposed model defines the properties of TI rocks in the local coordinate system. In the applications in which the global coordinate system is different from that of local coordinate system, the problem is solved in the local coordinate system and the solution in the global coordinate system can be obtained with the transition of the two coordinate systems.

The model is applicable to describing shear plastic deformation of TI rocks. For describing the tensile plastic deformation of TI rocks, different yielding criterion and plastic flow rule would be suggested.

Methodology for Parameter Determination

Elastic Parameters

The elastic parameters can be determined by combining triaxial compression tests of horizontal and vertical bedding specimens with a torsion test. Fig. 3 shows the local coordinate systems for horizontal and vertical bedding specimens used in the triaxial compression tests. A triaxial compression test of a horizontal bedding specimen in the elastic loading or unloading process would give the values of E_v and ν_{vh}, whereas a triaxial compression test of a vertical bedding specimen in the elastic loading or unloading process would give the values of E_h and ν_{hh}. Fig. 4 shows the schematic diagram of the torsion test for determination of G_{vh}. The torque is applied in the direction perpendicular to bedding planes in a horizontal bedding specimen. In the elastic domain, the value of the shear modulus of the rocks G_{vh} will be determined.

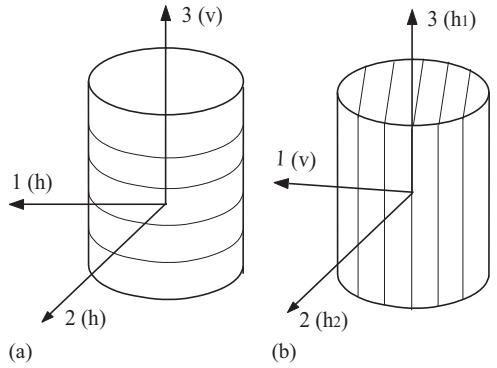

Fig. 3. Local coordinate systems for the horizontal (a) and vertical (b) bedding specimens

Determination of E_v and V_{vh}

For a horizontal bedding specimen in the local coordinate system shown in Fig. 3(a), the constitutive equation can be simplified from Eq. (1) as

$$\begin{bmatrix} \Delta\varepsilon_v^e \\ \Delta\varepsilon_h^e \end{bmatrix} = \begin{bmatrix} \frac{1}{E_v} & -\frac{2\nu_{vh}}{E_v} \\ -\frac{\nu_{vh}}{E_v} & \frac{(1-\nu_{hh})}{E_h} \end{bmatrix} \begin{bmatrix} \Delta\sigma_v \\ \Delta\sigma_h \end{bmatrix} \quad (10)$$

When conventional triaxial compression tests are performed, the confining pressure will be a constant, namely, $\Delta\sigma_h = 0$, and the following equations can be obtained using Eq. (10):

$$E_v = \frac{\Delta\sigma_v}{\Delta\varepsilon_v^e} \quad (11)$$

$$\nu_{vh} = -\frac{\Delta\varepsilon_h^e}{\Delta\varepsilon_v^e} \quad (12)$$

Determination of E_h and V_{hh}

For the vertical bedding, in the local coordinate system shown in Fig. 3(b), the constitutive equation becomes

$$\begin{bmatrix} \Delta\varepsilon_v^e \\ \Delta\varepsilon_{h2}^e \\ \Delta\varepsilon_{h1}^e \end{bmatrix} = \begin{bmatrix} \frac{1}{E_v} & -\frac{\nu_{vh}}{E_v} & -\frac{\nu_{vh}}{E_v} \\ -\frac{\nu_{vh}}{E_v} & \frac{1}{E_h} & -\frac{\nu_{hh}}{E_h} \\ -\frac{\nu_{vh}}{E_v} & -\frac{\nu_{hh}}{E_h} & \frac{1}{E_h} \end{bmatrix} \begin{bmatrix} \Delta\sigma_v \\ \Delta\sigma_{h2} \\ \Delta\sigma_{h1} \end{bmatrix} \quad (13)$$

The confining pressure is constant in a triaxial compression test, namely, $\Delta\sigma_v = \Delta\sigma_{h2} = 0$; thus, the following equations can be obtained using Eq. (13):

$$E_h = \frac{\Delta\sigma_{h2}}{\Delta\varepsilon_{h1}^e} \quad (14)$$

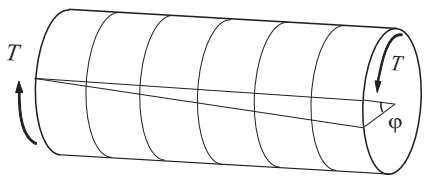

Fig. 4. Schematic diagram of the torsion test to determine G_{vh}

$$\nu_{hh} = -\frac{\Delta\varepsilon^e_{h2}}{\Delta\varepsilon^e_{h1}} \tag{15}$$

When a cylindrical specimen shown in Fig. 3(b) is tested in the triaxial compression test, ε^e_{h2} and ε^e_v cannot be measured separately and only the radial elastic strain ε^e_r can be measured. Because radial strain is defined as the average ratio of the specimen cross section before and after deformation, a relationship between radial strain and ε_{h2} and ε_v is found as

$$\pi\left[r(1+\varepsilon_{h2}) \times r(1+\varepsilon_v)\right] = \pi[r(1+\varepsilon_r)]^2 \tag{16}$$

that is

$$\Delta\varepsilon_r = (\Delta\varepsilon_{h2} + \Delta\varepsilon_v)/2 \tag{17}$$

$$\Delta\varepsilon^e_r = \left(\Delta\varepsilon^e_{h2} + \Delta\varepsilon^e_v\right)/2 \tag{18}$$

$$\Delta\varepsilon^p_r = \left(\Delta\varepsilon^p_{h2} + \Delta\varepsilon^p_v\right)/2 \tag{19}$$

In a triaxial compression test, $\Delta\sigma_v = \Delta\sigma_{h2} = 0$, and the following equation can be obtained using Eq. (13):

$$\Delta\varepsilon^e_v = -\frac{\nu_{vh}}{E_v} \cdot \Delta\sigma_{h1} \tag{20}$$

The following equation can be obtained combining Eqs. (18) and (20):

$$\Delta\varepsilon^e_{h_2} = 2\Delta\varepsilon^e_r + \frac{\nu_{vh}}{E_v} \cdot \Delta\sigma_{h1} \tag{21}$$

The following equation is obtained when Eq. (21) is substituted into Eq. (15):

$$\nu_{hh} = -\frac{2\Delta\varepsilon^e_r}{\Delta\varepsilon^e_{h1}} - \nu_{vh} \cdot \frac{E_h}{E_v} \tag{22}$$

Therefore, E_v and ν_{vh} can be determined using the test of a horizontal bedding specimen, and E_h and ν_{hh} can be determined using the tests of both horizontal and vertical bedding specimens as expressed in Eqs. (14) and (22).

Determination of G_{vh}

A torsion test of a horizontal bedding specimen can be used to determine G_{vh} as shown in Fig. 4. The shear modulus G can be calculated using the shear formula of Hooke's law when the material is in torsion

$$G_{vh} = \frac{TL}{I_p \phi} \tag{23}$$

where G_{vh} = shear modulus perpendicular to the isotropic plane; T = applied torque; L = length of the specimen; ϕ = rotation angle; and I_p = polar moment of inertia.

Plastic Parameters

Constraint on Plastic Parameters

Fig. 5 shows a plane element of anisotropic material subjected to pure shear stress τ_{xy}, at which the yielding of material starts. With Eq. (3), it is obtained that

$$\sqrt{2N(\tau_{xy})^2} = D \tag{24}$$

When the coordinate system is rotated 45° clockwise, the principal stress space is obtained, in which the principal stresses are τ_{12} and $-\tau_{12}$, respectively. Substituting the stress components into Eq. (3), it is obtained that

$$\sqrt{(F+G+4H)(\tau_{xy})^2} = D \tag{25}$$

Comparison of Eq. (24) with Eq. (25) gives

$$2N = F + G + 4H \tag{26}$$

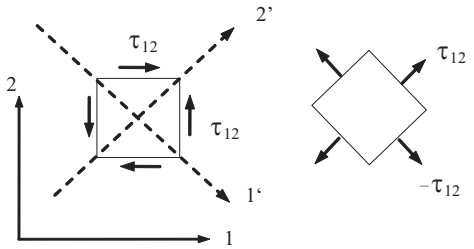

Fig. 5. Transformation of stress states of a plane element of a material subjected to pure shear stresses at which yielding starts to occur: 1 and 2 are coordinate axes before transformation; 1′ and 2 are coordinate axes after transformation

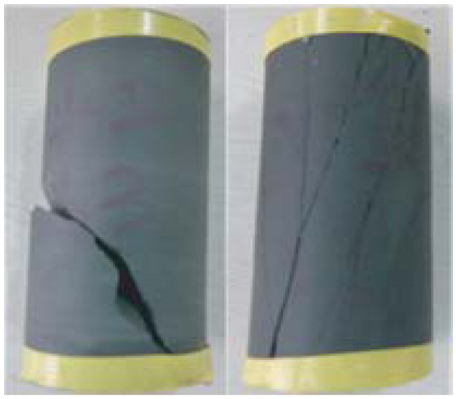

(a)

(b)

Fig. 6. Failure of specimens in the triaxial compression (a) and torsion (b) tests

In the same manner, the following relations will be obtained:

$$2L = 4F + G + H \tag{27}$$

$$2M = F + 4G + H \tag{28}$$

The relations expressed by Eqs. (26)–(28) lay the constraint on the plastic parameters for the TI plastic model.

Determination of F, H, and N

For a triaxial compression test on a horizontal bedding specimen, as shown in Fig. 3(a), $\sigma_{11} = \sigma_{22}$; therefore, the following equations are derived from the plastic potential:

$$\frac{\partial f(\sigma)}{\partial \sigma_{11}} = \frac{\partial f(\sigma)}{\partial \sigma_{22}} = \frac{F}{f(\sigma)}(\sigma_{11} - \sigma_{33}) - \alpha \tag{29}$$

$$\frac{\partial f(\sigma)}{\partial \sigma_{33}} = -\frac{2F}{f(\sigma)}(\sigma_{11} - \sigma_{33}) - \alpha \tag{30}$$

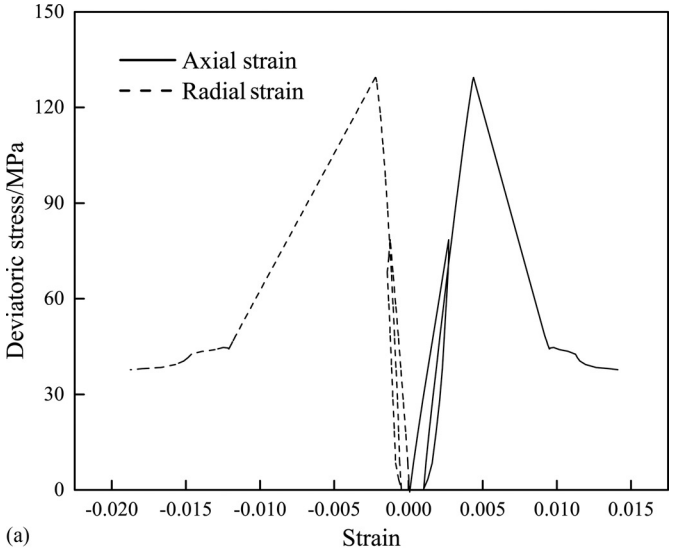

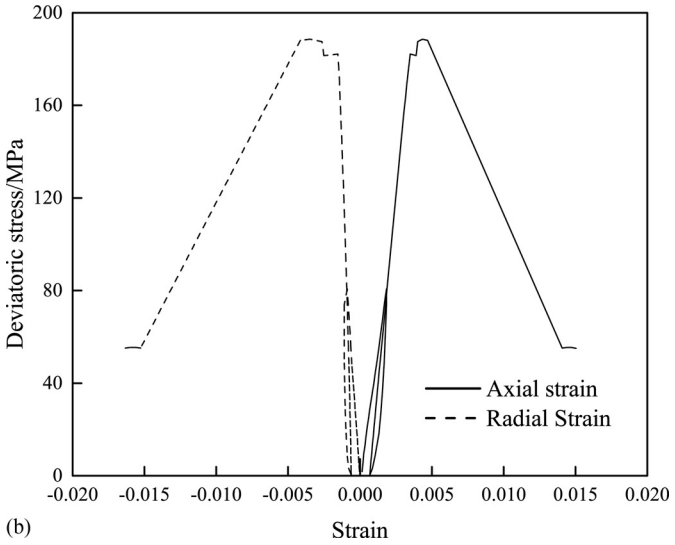

Fig. 7. Deviatoric stress versus axial and radial strain relations of horizontal (a) and vertical (b) bedding specimens in triaxial compression under the confining pressure of 5 MPa

The radial plastic strain increment is expressed as

$$d\varepsilon_r^p = d\varepsilon_{11}^p = d\varepsilon_{22}^p = d\lambda \frac{\partial f(\sigma)}{\partial \sigma_{11}} = d\lambda \left[\frac{F}{f(\sigma)}(\sigma_{11} - \sigma_{33}) - \alpha \right] \tag{31}$$

and the axial plastic strain increment is expressed as

$$d\varepsilon_a^p = d\varepsilon_{33}^p = d\lambda \frac{\partial f(\sigma)}{\partial \sigma_{33}} = d\lambda \left[-\frac{2F}{f(\sigma)}(\sigma_{11} - \sigma_{33}) - \alpha \right] \tag{32}$$

Regarding on the test of the vertical bedding specimen, as shown in Fig. 3(b), $\sigma_{22} = \sigma_{33}$, so

$$\frac{\partial f(\sigma)}{\partial \sigma_{11}} = \frac{F + H}{f(\sigma)}(\sigma_{11} - \sigma_{33}) - \alpha \tag{33}$$

$$\frac{\partial f(\sigma)}{\partial \sigma_{22}} = -\frac{H}{f(\sigma)}(\sigma_{11} - \sigma_{33}) - \alpha \tag{34}$$

$$\frac{\partial f(\sigma)}{\partial \sigma_{33}} = -\frac{F}{f(\sigma)}(\sigma_{11} - \sigma_{33}) - \alpha \tag{35}$$

The radial plastic strain increment is expressed as

$$\begin{aligned} d\varepsilon_r^p &= \frac{1}{2}\left(d\varepsilon_{22}^p + d\varepsilon_{33}^p\right) = \frac{1}{2}\left(d\lambda \frac{\partial f(\sigma)}{\partial \sigma_{22}} + d\lambda \frac{\partial f(\sigma)}{\partial \sigma_{33}}\right) \\ &= d\lambda \left[-\frac{F + H}{2f(\sigma)}(\sigma_{11} - \sigma_{33}) - \alpha \right] \end{aligned} \tag{36}$$

and the axial plastic strain increment is expressed as

$$d\varepsilon_a^p = d\varepsilon_{11}^p = d\lambda \frac{\partial f(\sigma)}{\partial \sigma_{11}} = d\lambda \left[\frac{F + H}{f(\sigma)}(\sigma_{11} - \sigma_{33}) - \alpha \right] \tag{37}$$

The plastic strains could be obtained by subtracting the elastic strains from the strains. The parameter α is determined in triaxial compression tests on the specimens under different

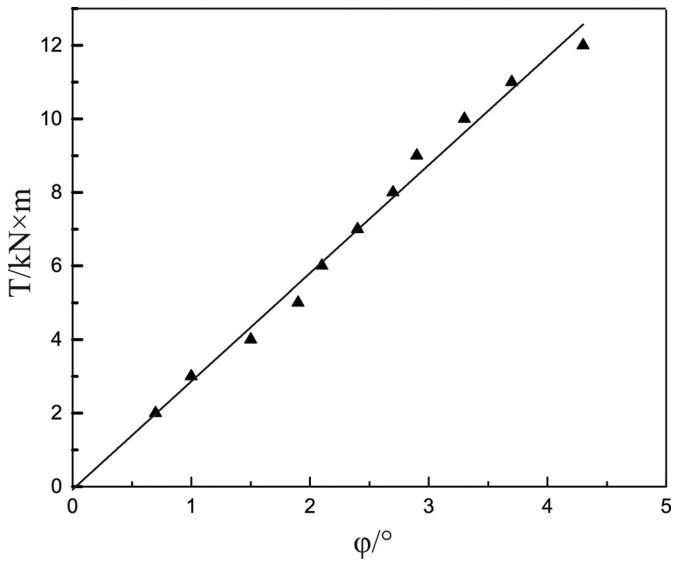

Fig. 8. Torque versus rotation angle relation of a horizontal bedding specimen in the torsion test

confining pressures. The parameters for the plastic potential, i.e., F, H, and N, could be determined by combining Eqs. (31), (32), and (36).

Along with using the relation of Eq. (26), parameter N can also be determined using Eq. (5). The shear strain increment could be expressed as

$$d\varepsilon_{12}^{p} = d\lambda \frac{\partial f(\sigma)}{\partial \sigma_{12}} = d\lambda \left[\frac{4N\sigma_{12}}{f(\sigma)}\right] \tag{38}$$

Table 1. TI Elastic Parameters of Carbonaceous Slate

Parameter	Value
E_v/MPa	46,095
E_h/MPa	64,500
ν_{vh}	0.35
ν_{hh}	0.16
G_{vh}/MPa	18,534

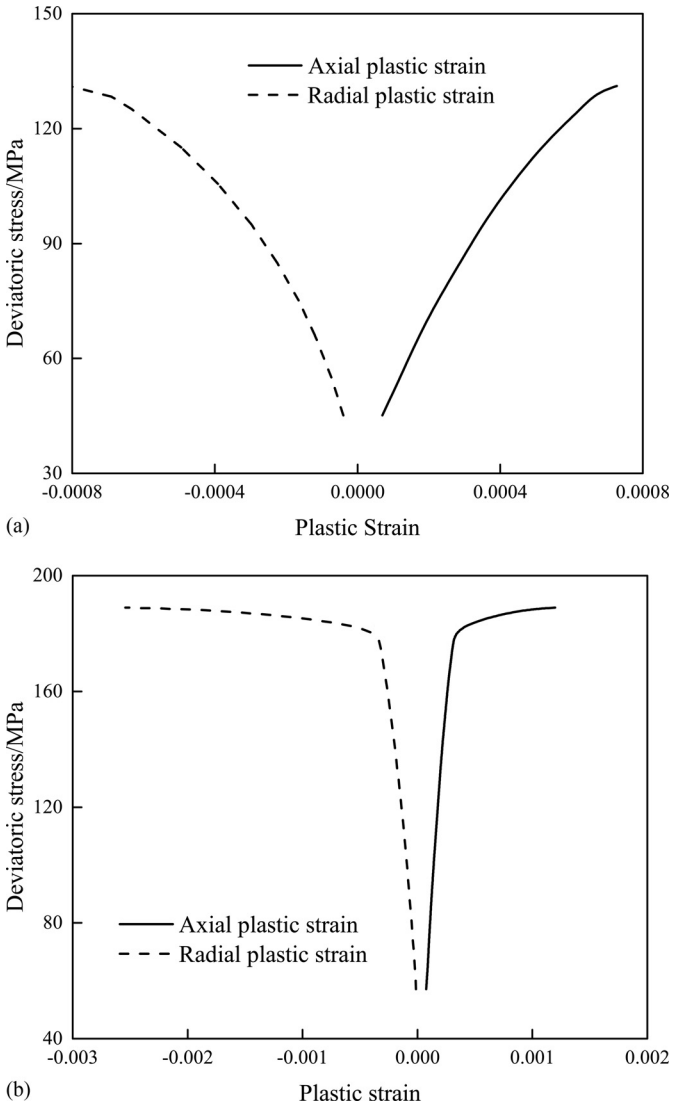

Fig. 9. Deviatoric stress versus axial and radial plastic strain relations of horizontal (a) and vertical (b) bedding specimens in triaxial compression under the confining pressure of 5 MPa

Eq. (38) could be used to verify the parameters determined using the previously described method.

Yield Parameters

Two parameters in the yield function, β and D, can be obtained by determining the yield stresses under different confining pressures in the triaxial compression tests, whereas the values of the other two parameters i.e., F and H, are identical to those determined in the previous section.

Hardening Parameters

The relationship between plastic strain and stress can be prescribed as a function or a tabulated data set (SIMULIA 2006). In this study, the latter method is adopted.

Verification of the Model and Methodology

Test Methods

In this study, the conventional triaxial compression tests were performed using an RLW-500 microcomputer-controlled rock

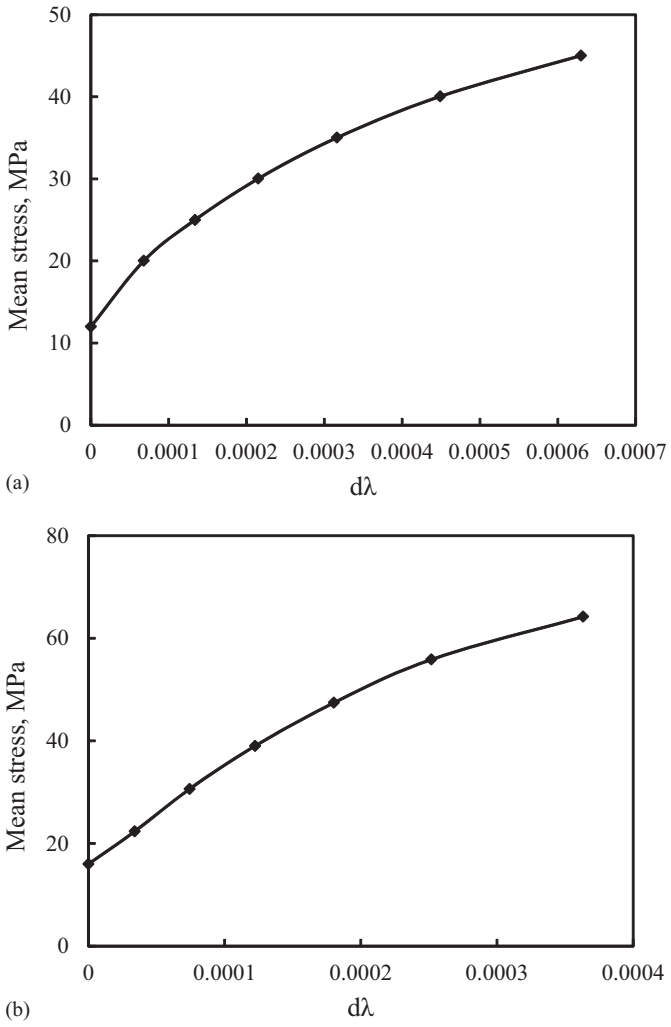

Fig. 10. Relations between mean stress and plastic factor for the horizontal (a) and vertical (b) bedding specimens

triaxial testing system. The system has the following parameters: a maximum axial load of 1,000 kN, with an accuracy of 1%; a maximum radial pressure of 50 MPa, with an accuracy of ±2%; and a maximum axial deformation of 10 mm and a maximum radial deformation of 5 mm, with accuracies of ±0.5%.

Table 2. TI Plastic Parameters of Carbonaceous Slate

Parameter	Value
β	0.13
D/MPa	11
α	0.17
F	0.59
H	0.37
N	1.33

Carbonaceous slate specimens were made out of core samples from the rock mass around the Muzhailing Tunnel in northwestern China. The core samples were prepared carefully to obtain the horizontal and vertical beddings specimens. The diameter of the specimens was 50 mm and the height was 100 mm.

In triaxial compression tests, the confining pressure was 5 MPa. Figs. 3 (a and b) illustrate the specimens with bedding planes. In the test, the loading rate of confining pressure was kept at 0.05 MPa/s, and the axial load was 100 N/s. Unloading and reloading processes were performed in the tests to determine the elastic parameters of the carbonaceous slate. It was assumed that the specimens exhibited elastic behavior in unloading or reloading processes. In the torsion test, a K-50 torsion testing

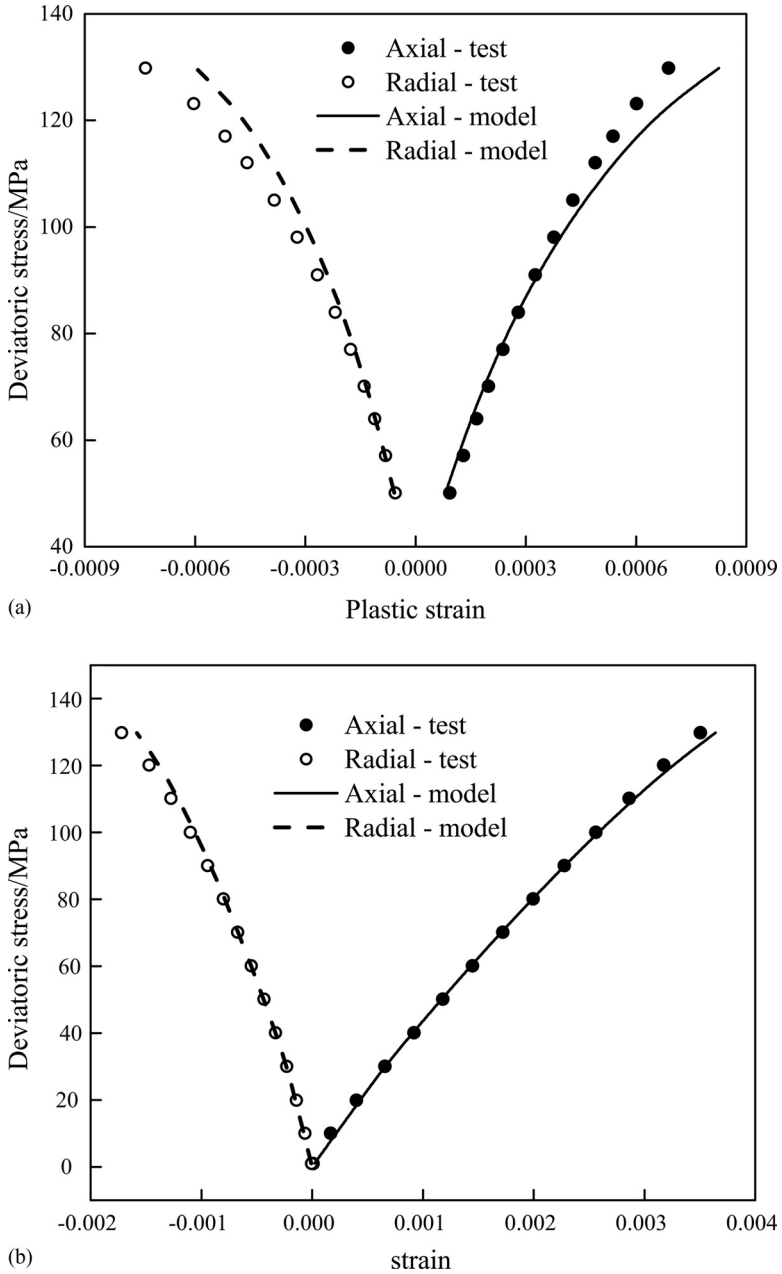

Fig. 11. Comparison between tested and predicted deviatoric stress versus plastic strain (a) and strain (b) relations of horizontal bedding specimen in triaxial compression under the confining pressure of 5 MPa

system was used. Special molds were designed and manufactured to mount the specimen on the equipment. A specimen with horizontal bedding was used in the test, as shown in Fig. 4. The molds and the specimens were spliced using high-strength epoxy resin. Fig. 6 shows the failure of specimens in the triaxial compression and torsion tests.

Test Results

Fig. 7(a) shows the deviatoric stress versus axial and radial strain and relations of the horizontal specimen under a confining pressure of 5 MPa. It shows that the sample experienced strain-hardening behavior before the peak and then strain-softening behavior after the peak. However, the strain-hardening behavior is of interest in this study. The specimen failed at the deviatoric stress of 131 MPa, and the residual strength of the specimen is 40 MPa.

Fig. 7(b) shows the deviatoric stress versus axial strain and radial strain relations of the vertical bedding specimens under a confining pressure of 5 MPa. It shows that a significant strain-softening phenomenon occurs in both axial and radial directions. The specimen failed at the deviatoric stress of 188 MPa, and the residual strength of the specimen is 56 MPa. Both peak strength and residual strength of the vertical bedding specimen are higher than those of the horizontal bedding specimen.

Fig. 8 shows the torque versus rotation angle relation in the reloading process in the torsion test. A linear relationship between the torque and rotation angle appears in the torque up to 12 kN · m.

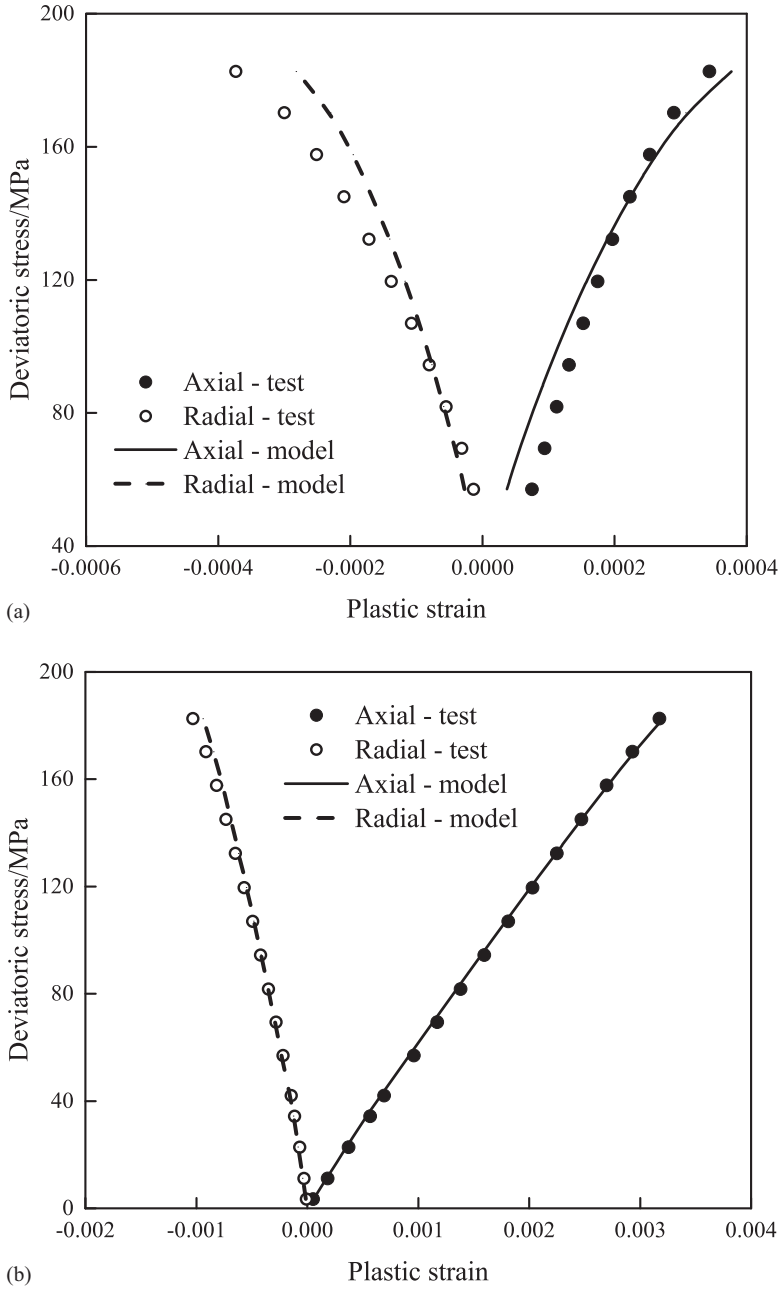

Fig. 12. Comparison between tested and predicted deviatoric stress versus plastic strain (a) and strain (b) relations of vertical bedding specimens in triaxial compression under the confining pressure of 5 MPa

It was supposed that the specimen exhibited elastic behavior in the range of shear stress applied in the test.

Determination of Parameters

To determine the elastic and plastic parameters, the strain should be decomposed into elastic and plastic strains. In this study, it is assumed that an unloading process is reversible and the specimens exhibit elastic behavior in an unloading process. It is also assumed that the elastic modulus is the same in both unloading and reloading processes for TI rocks.

Elastic Parameters

From the triaxial compression tests, E_v and v_{vh} were determined using the relations in the unloading processes with Eqs. (11) and (12), respectively. E_h and v_{hh} were determined in the unloading processes with Eqs. (14) and (15), and G_{vh} was determined using Eq. (23). The determined elastic parameters are shown in Table 1. The carbonaceous slate is featured with TI property. The anisotropy ratio for elasticity, defined as the ratio of E_h over E_v, is 1.4.

Plastic Parameters

Using the elastic parameters in Table 1, the axial and radial elastic strains of the horizontal and vertical specimens were calculated using Eq. (1) in the triaxial compression tests. In this manner, the plastic strains of the specimens in axial and radial directions were calculated.

Fig. 9(a) shows the deviatoric stress versus axial and radial plastic strain relations of the horizontal specimens. With the increase of the deviatoric stress, both the axial and radial plastic strains increase with an increase in the deviatoric stress. It is noted that the axial and radial plastic strain is nearly the same for this specimen in the test, although the axial strain is higher than radial strain for a specified deviatoric stress, as shown in Fig. 7(a). It could be induced because the elastic modulus perpendicular to the bedding planes, E_v, is lower than the elastic modulus in the bedding planes, E_h. Fig. 9(b) shows the deviatoric stress versus axial and radial plastic strain of the vertical bedding specimen. The axial and radial plastic strains both increase with deviatoric stress, and the strain rate increases with the increase of the deviatoric stress. When approaching the peak strength, the rates of axial and radial plastic strains attained the maximum values.

Figs. 10(a and b) show the relations between mean stress and plastic factor for the horizontal and vertical bedding specimens. These two relations are used to specify the hardening property of the rock specimens.

As measured by the tests, the internal friction angle of the carbonaceous slate is 32.5°; thus, α was determined as 0.17 according to Eq. (9). Then F and H were determined with Eqs. (31), (32), and (36). Finally, N was calculated with Eq. (26). The resulting plastic parameters of the carbonaceous slate of the constitutive model are shown in Table 2. The anisotropic ratio for plasticity, which is defined as the ratio of F over H, is 1.6. The specimen shows the strong dependency of plastic property on the loading direction.

Comparison between Test Data and Model Prediction

Fig. 11 shows the comparison between tested and predicted deviatoric stress versus plastic strain and strain relations of the horizontal bedding specimen in the triaxial compression test. Fig. 12 shows the comparison between tested and predicted deviatoric stress versus plastic strain and strain relations of the vertical bedding specimen in the triaxial compression test. It can be seen from the comparisons that the model predictions are in good agreement with the test results, indicating that the existing model and the model parameters can well describe the TI behavior of carbonaceous slates.

Discussions

Plastic Flow Directions

Fig. 13 compares the volumetric plastic strain versus axial plastic strain relations of the horizontal and vertical bedding specimens. A compressive strain is positive, and a tensile strain is negative. Given a certain axial plastic strain, the volumetric plastic strain of the

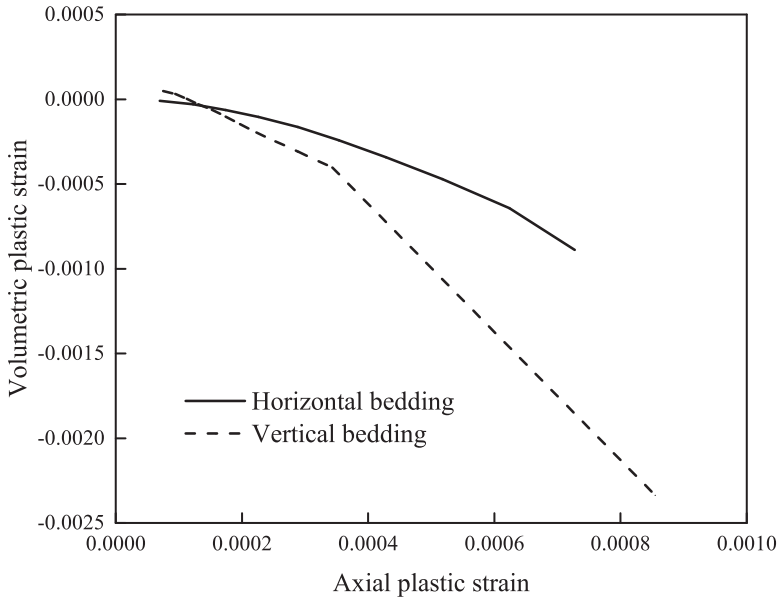

Fig. 13. Volumetric plastic strain versus axial plastic strain relations of horizontal and vertical bedding specimens in triaxial compression under the confining pressure of 5 MPa

horizontal bedding specimen is much smaller than that of the vertical bedding specimen. With the increase of the axial plastic strain, the volumetric plastic strain increases gradually.

Potential has been used to describe the flow direction of rock in the constitutive modeling of rock behavior. It is significant to compare the potentials of the horizontal and vertical bedding specimens. In Figs. 14(a and b), the directions of plastic flow are represented using some vectors. The locations of the vectors in stress space are defined by the stress states. The directions of the vectors are defined by the ratio of plastic shear strain and plastic volumetric strain increments. The inclined angles of the vectors are usually termed as dilation angle. The dilation angle increases with the stresses applied on specimens. At an identical stress state, the dilation angle for the vertical bedding specimen is higher than that of the horizontal bedding specimen, which means that the plastic potential is dependent on the loading direction.

Elastic and Plastic Parameters Interaction

In the earlier analysis, the plastic parameters were determined based on the decomposition of strains. Variations in elastic parameters would alter the parameters for plasticity. It is interesting and useful to investigate the sensitivity of plastic parameters to the variation of elastic parameters. The effect of the variations in elastic parameters E_v and v_{vh} on the plastic potential is discussed using the test data of the horizontal bedding specimen. The results are shown in Fig. 15, which shows that the dilation angle increases with both the elastic modulus E_v and Poisson's ratio v_{vh}.

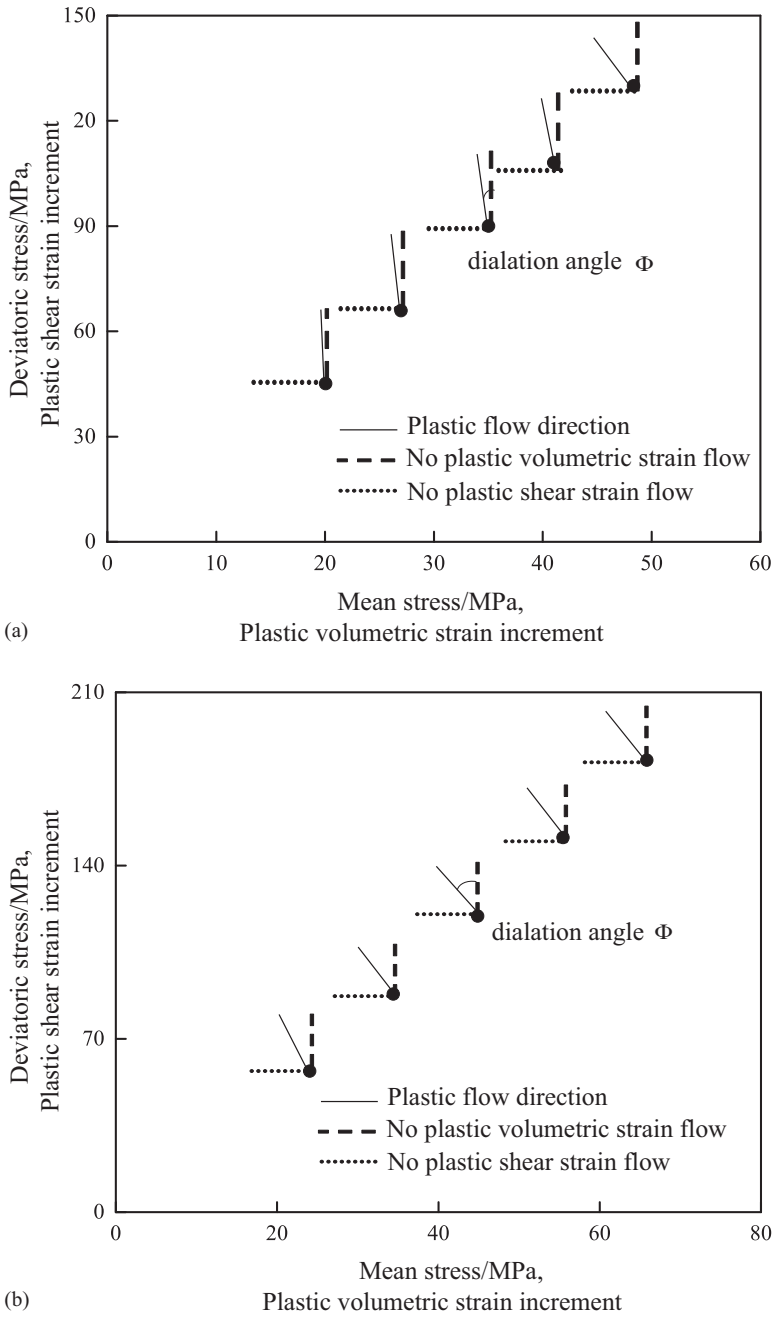

Fig. 14. Plastic strain increments in the stress space for horizontal (a) and vertical (b) bedding specimens in triaxial compression under the confining pressure of 5 MPa

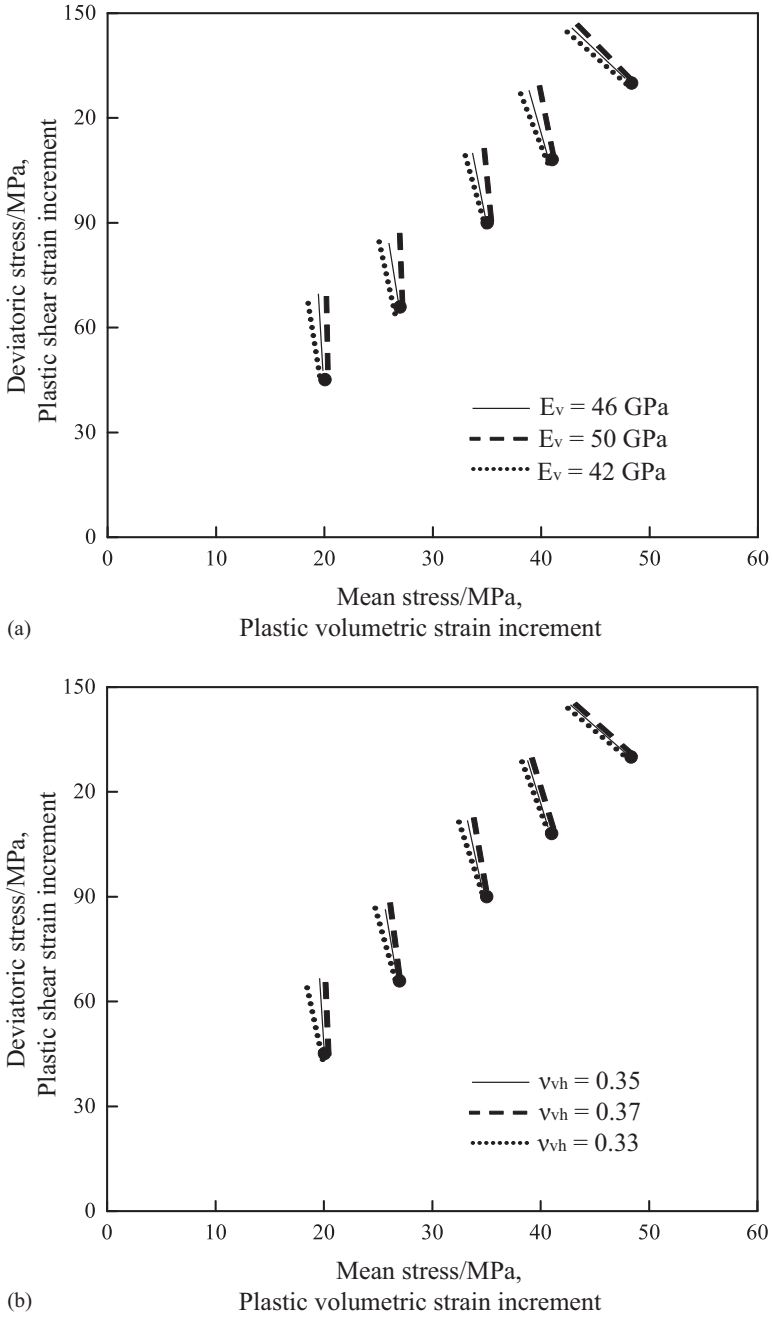

Fig. 15. Effect of elastic parameters (a) E_v and (b) ν_{vh} on plastic flow directions at different stress states for the horizontal bedding specimen

Dependency of Strength on Loading Direction

Quite a few studies (Tien et al. 2006; Singh et al. 2015; Shi et al. 2016) have been performed to investigate the dependency of triaxial compression strength on loading direction. It was found that the strength varies with the loading direction in a nonlinear manner. In this section, the proposed model was used to investigate the dependency with the triaxial compression test data on phyllite reported in Singh et al. (2015). The axial stresses at failure of the specimens with different dip angles of the bedding plane in triaxial compression tests with the confining pressures of 5 and 30 MPa are tabulated in Table 3, in which θ is the inclination angle of the normal direction of the bedding planes.

Fig. 16 shows the coordinate systems associated with the specimen in triaxial compression tests. The stress components in the coordinate system 1'2'3 were obtained using the stress transformation formula

$$\sigma_{11} = \frac{1}{2}(\sigma_1 + \sigma_3) + \frac{1}{2}(\sigma_1 - \sigma_3)\cos 2\theta \tag{39}$$

$$\sigma_{22} = \frac{1}{2}(\sigma_1 + \sigma_3) - \frac{1}{2}(\sigma_1 - \sigma_3)\cos 2\theta \tag{40}$$

$$\sigma_{33} = \sigma_3 \tag{41}$$

The substitution of the previously mentioned stress components into Eq. (5) leads to the following equation:

Table 3. Axial Stresses at Failure (in Megapascals) of Phyllite Specimens with Different Bedding Directions When Subjected to Different Confining Pressures (Data from Singh et al. 2015)

	β						
σ_3 (MPa)	0°	15°	30°	45°	60°	75°	90°
5	110	80	48	51	65	100	110
30	210	170	130	120	155	200	220

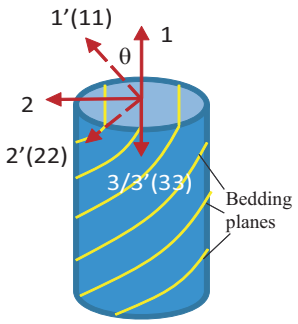

Fig. 16. Coordinate systems associated with the specimen: 1, 2, and 3 are coordinate axes along the first, second, and third principle stress directions; 1′ is the coordinate axis along the normal direction of bedding planes; 2′ and 3′ are coordinate axes in bedding planes in which the coordinate axes 3′ and 3 are coincident one another

Table 4. TI Strength Parameters of the Models for the Phyllite in Triaxial Compression Tests

Model	α	D/MPa	F	H
This study	0.5	45	4.8	–3.8
DP	0.707	56.56	—	—
Hill	—	127.3	4.8	–3.8

$$\sigma_1 = \frac{D}{X-\beta} + \frac{2\beta + X}{X-\beta}\sigma_3 \tag{42}$$

in which, X is a coefficient related to loading direction and it is expressed as

$$X = \sqrt{\left\{F\left[\frac{1}{2}(1-\cos 2\theta)\right]^2 + F\left[\frac{1}{2}(1+\cos 2\theta)\right]^2 + H(\cos 2\theta)^2\right\}} \tag{43}$$

Fitting Eq. (42) with the test data in Table 3 yielded the parameters in Table 4. The DP model and Hill's model were fitted with the test data in Table 3. The parameters of these two models are presented in Table 4. The comparison between test data and model predictions is shown in Fig. 17.

It is interesting to note that Hill's model could predict the loading direction-dependent strength with a limited range. The comparison indicates that the proposed model in this study could describe the dependency of triaxial compression strength on both loading direction and confining pressure.

Conclusions

In this paper, the elastoplastic property of TI rock was analyzed and a constitutive model for the property was proposed. The methodology for parameter determination was developed. The proposed model and the parameter determination methodology were applied to modeling the TI elastoplastic property of carbonaceous slate in triaxial compression.

A TI elastoplastic model for rocks was proposed. In the model, the generalized Hooke's law was adopted for the elastic behavior. For the plastic behavior, the yield criterion and plastic potential are formulated as functions of the generalized octahedral shear stress and the first invariant of stress tensor. A nonassociated flow rule and a stress-dependent hardening rule were adopted in the model. The plastic model can be simplified to the DP model for isotropic rocks. A methodology for the model

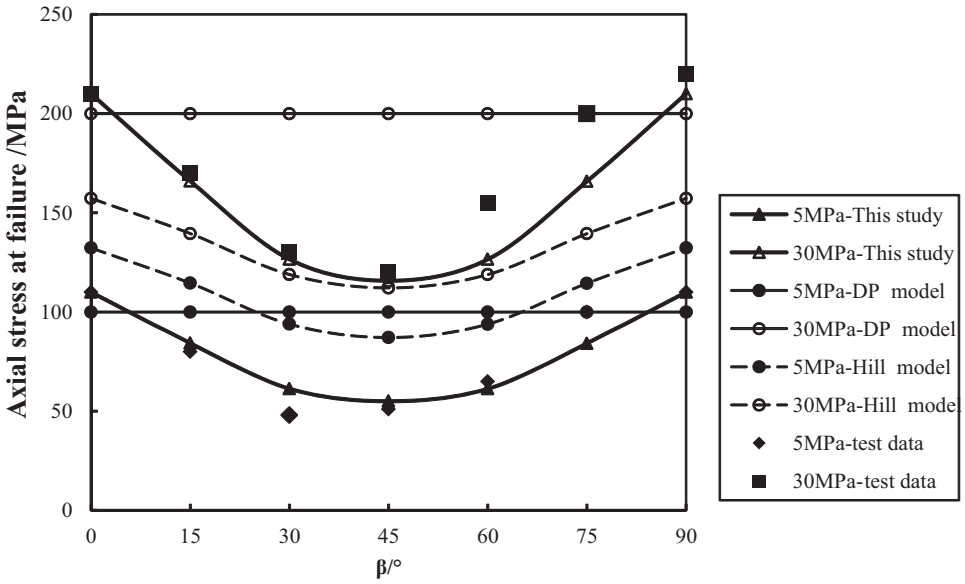

Fig. 17. Comparison of the triaxial compression strength between the test data (Singh et al. 2015) and predictions from DP, Hill, and extended Hill models

parameter determination was developed. The parameters can be determined by combining triaxial compression tests with a torsion test on specimens with different bedding directions. The constraint on plastic parameters was theoretically identified.

The proposed model and the parameter determination methodology were applied to modeling the TI elastoplastic property of carbonaceous slate in triaxial compression. The results show that the model proposed in this study can well describe the transverse isotropic elastoplastic property of the rock, and the parameter determination methodology is simple and effective. Several other issues including the plastic flow directions, the interaction between elastic and plastic parameters, and the dependency of strength on loading direction were also discussed. It was found that at an identical stress state, the dilation angle for the vertical bedding specimen is higher than that of the horizontal bedding specimen due to the dependency of plastic flow on loading direction. The dilation angle increases with both the elastic modulus E_v and Poisson's ratio v_{vh}. The proposed model could describe the dependency of triaxial compression strength on both loading direction and confining pressure.

In this study, a framework on the constitutive modeling of TI elastoplastic property of rocks and parameter determination has been developed. The framework could be extended to modeling other geomaterials exhibiting TI property. In practice, careful preparation of the specimens and an adequate number of tests are recommended for the application of the framework.

Acknowledgments

The authors acknowledge the financial support from the National Natural Science Foundation of China (grant numbers 51579141 and 51309145), and the Open Research Fund of the State Key Laboratory of Geomechanics and Geotechnical Engineering, Institute of Rock and Soil Mechanics, Chinese Academy of Sciences, under Grant No. Z011005.

Notation

The following symbols are used in this paper:

E_h = elastic modulus in the isotropic plane;
E_v = elastic modulus in the direction perpendicular to the isotropic plane;
F = plastic potential;
F, G, H, L, M, N = parameters in the yield function of Hill's model;
G = yield function;
G_{vh} = shear modulus in the direction perpendicular to the isotropic plane;
I_p = polar moment of inert;
I_1 = first invariant of stress tensor;
L = length of specimen;
T = torque in torsion test;
ν_{hh} = Poisson's ratio in the isotropic plane;
ν_{vh} = Poisson's ratio, which is the ratio of the strain in the isotropic plane over that in the direction perpendicular to the isotropic plane;
α = parameter in plastic potential of the extended Hill's model;
β and D = parameters in the yield function of the extended Hill's model;
ε_{ij}^p = plastic strain component;
$\varepsilon_v, \varepsilon_h, \varepsilon_{h1}, \varepsilon_{h2}, \varepsilon_a, \varepsilon_r$ = stress tensor components in triaxial compression tests
$\varepsilon_{11}, \varepsilon_{22}, \varepsilon_{33}, \gamma_{23}, \varepsilon_{31}\varepsilon_{12}$ = strain tensor components in local coordinate system;
θ = dip angle of bedding planes of specimens in triaxial compression;
$\sigma_v, \sigma_h, \sigma_{h1}, \sigma_{h2}$ = stress tensor components in triaxial compression tests;
$\sigma_{xx}, \sigma_{yy}, \sigma_{zz}, \tau_{yz}, \tau_{zx}, \tau_{xy}$ = stress tensor components in global coordinate system;
$\sigma_{11}, \sigma_{22}, \sigma_{33}, \tau_{23}, \tau_{31}\tau_{12}$ = stress tensor components in local coordinate system; and
φ = dilation angle;
ϕ = rotation angle.

References

Amadei, B. (1996). "Importance of anisotropy when estimating and measuring in situ stresses in rock." *Int. J. Rock Mech. Min. Sci. Geomech.*, 33(3), 293–325.
Anandarajah, A. (2008). "Multi-mechanism anisotropic model for granular materials." *Int. J. Plast.*, 24(5), 804–846.
Barton, N., and Quadros, E. (2015). "Anisotropy is everywhere, to see, to measure, and to model." *Rock Mech. Rock Eng.*, 48(4), 1323–1339.
Bobet, A. (2011). "Lined circular tunnels in elastic transversely anisotropic rock at depth." *Rock Mech. Rock Eng.*, 44(2), 149–167.
Chang, J., Chu, X., and Xu, Y. (2015). "Finite-element analysis of failure in transversely isotropic geomaterials." *Int J. Geomech*, 10.1061/(ASCE)GM.1943-5622.0000455, 04014096.
Chou, Y.-C., and Chen, C.-S. (2008). "Determining elastic constants of transversely isotropic rocks using Brazilian test and iterative procedure." *Int. J. Numer. Anal. Methods Geomech.*, 32(3), 219–234.
Ding, H., Chen, W., and Zhang, L. (2006). *Elasticity of transversely isotropic materials*, Springer Science & Business Media, Dordrecht, Netherlands.
Exadaktylos, G. E. (2001). "On the constraints and relations of elastic constants of transversely isotropic geomaterials." *Int. J. Rock Mech. Min. Sci.*, 38(7), 941–956.
Gao, C. Y., Xu, J., Li, Z.-H., and Deng, J. H. (2011). "Experimental study of anisotropically mechanical characteristics of sandy slate in Xuefeng mountain tunnel." *Rock Soil Mech.*, 32(5), 1360–1364 (in Chinese).
Gautam, R., and Wong, R. C. K. (2006). "Transversely isotropic stiffness parameters and their measurement in Colorado shale." *Can. Geotech. J.*, 43(12), 1290–1305.
Hakala, M., Kuula, H., and Hudson, J. A. (2007). "Estimating the transversely isotropic elastic intact rock properties for in situ stress measurement data reduction: A case study of the Olkiluoto mica gneiss, Finland." *Int. J. Rock Mech. Min. Sci.*, 44(1), 14–46.
Hefny, A. M., and Lo, K. Y. (1999). "Analytical solutions for stresses and displacements around tunnels driven in cross-anisotropic rocks." *Int. J. Numer. Anal. Methods Geomech.*, 23(2), 161–177.
Hill, R. (1950). *The mathematical theory of plasticity*, Clarendon Press, Oxford, U.K.
Huang, S., and Khan, A. S. (1991). "An analysis of finite elastic-plastic deformation under biaxial compression." *Int. J. Plast.*, 7(3), 219–234.
Kamrin, K. (2010). "Nonlinear elasto-plastic model for dense granular flow." *Int. J. Plast.*, 26(2), 167–188.

Khan, A. S., Xiang, Y., and Huang, S. (1991). "Behavior of Berea sandstone under confining pressure part I: Yield and failure surfaces, and nonlinear elastic response." *Int. J. Plast.*, 7(6), 607–624.
Khan, A. S., Xiang, Y., and Huang, S. (1992). "Behavior of Berea sandstone under confining pressure part II: Elastic-plastic response." *Int. J. Plast.*, 8(3), 209–220.
Lai, Y., Jin, L., and Chang, X. (2009). "Yield criterion and elasto-plastic damage constitutive model for frozen sandy soil." *Int. J. Plast.*, 25(6), 1177–1205.
Liu, Y., Fu, H., Wu, Y., Rao, J., Yin, Q., and Yuan, W. (2013). "Experimental study of elastic parameters and compressive strength for transversely isotropic rocks." *J. Cent. South Univ.*, 44(8), 3398–3404.
Long, N. M. A. N., Khaldjigitov, A. A., and Adambaev, U. (2013). "On the constitutive relations for isotropic and transversely isotropic materials." *Appl. Math. Modell.*, 37(14–15), 7726–7740.
Muraleetharan, K. K., Liu, C., Wei, C., Kibbey, T. C., and Chen, L. (2009). "An elastoplatic framework for coupling hydraulic and mechanical behavior of unsaturated soils." *Int. J. Plast.*, 25(3), 473–490.
Nixon, S. A., and Chandler, H. W. (1999). "On the elasticity and plasticity of dilatant granular materials." *J. Mech. Phys. Solids*, 47(6), 1397–1408.
Shao, J. F., and Henry, J. P. (1991). "Development of an elastoplastic model for porous rock." *Int. J. Plast.*, 7(1–2), 1–13.
Shen, W. Q., and Shao, J. F. (2016). "An incremental micro-macro model for porous geomaterials with double porosity and inclusion." *Int. J. Plast.*, 83(Aug), 37–54.
Shi, X., Yang, X., Meng, Y., and Gao, L. (2016). "An anisotropic strength model for layered rocks considering planes of weakness." *Rock Mech. Rock Eng.*, 49(9), 3783–3792.
Simanjuntak, T. D. Y. F., Marence, M., Schleiss, A. J., and Mynett, A. E. (2016). "The interplay of in situ stress ratio and transverse isotropy in the rock mass on prestressed concrete-lined pressure tunnels." *Rock Mech. Rock Eng.*, 49(11), 1–22.
SIMULIA. (2006). *Abaqus documentation, version 6.6*, SIMULIA, Providence, RI.
Singh, M., Samadhiya, N. K., Kumar, A., and Singh, B. (2015). "A nonlinear criterion for triaxial strength of inherently anisotropic rocks." *Rock Mech. Rock Eng.*, 48(4), 1387–1405.
Talesnick, M. L., Lee, M. Y., and Haimson, B. C. (1995). "On the determination of elastic material parameters of transverse isotropic rocks from a single test specimen." *Rock Mech. Rock Eng.*, 28(1), 17–35.
Tien, Y. M., Kuo, M. C., and Juang, C. H. (2006). "An experimental investigation of the failure mechanism of simulated transversely isotropic rocks." *Int. J. Rock Mech. Min. Sci.*, 43(8), 1163–1181.
Tsutsumi, S., and Hashiguchi, K. (2005). "General non-proportional loading behavior of soils." *Int. J. Plast.*, 21(10), 1941–1969.
Vorobiev, O. (2008). "Generic strength model for dry jointed rock masses." *Int. J. Plast.*, 24(12), 2221–2247.
Vu, T. M., Sulem, J., Subrin, D., and Monin, N. (2013a). "Semi-analytical solution for stresses and displacements in a tunnel excavated in transversely isotropic formation with non-linear behavior." *Rock Mech. Rock Eng.*, 46(2), 213–229.
Vu, T. M., Sulem, J., Subrin, D., Monin, N., and Lascols, J. (2013b). "Anisotropic closure in squeezing rocks: The example of Saint-Martin-la-Port Access Gallery." *Rock Mech. Rock Eng.*, 46(2), 231–246.
Wang, Y., Ding, W., Jia, S., and Zou, C. (2014). "Anisotropic model of layered rock mass considering characteristics of structural interface." *J. Highway Transp. Res. Dev.*, 31(10), 85–92 (in Chinese).
Wang, Z., and Wong, R. (2016). "Strain-dependent and stress-dependent creep model for a till subject to triaxial compression." *Int J. Geomech*, 10.1061/(ASCE)GM.1943-5622.0000670, 04016027.
Wang, Z. and Wong, R. (2017). "Strain-dependent creep behavior of Athabasca oil sand in triaxial compression." *Int J. Geomech.*, 10.1061/(ASCE)GM.1943-5622.0000583, 04015084.
Xu, L., Ren, Q., Du, X., and Ye, Z. (2010). "An anisotropic elastoplastic constitutive model for layered rock masses and its implementation." *Chinese J. Undergr. Sp. Eng.*, 6(4), 763–769 (in Chinese).
Yin, Z. Y., Chang, C. S., Hicher, P. Y., and Karstunen, M. (2009). "Micromechanical analysis of kinematic hardening in natural clay." *Int J. Plast.*, 25(8), 1413–1435.
Yin, Z. Y., Chang, C. S., Karstunen, M., and Hicher, P. Y. (2010). "An anisotropic elastic–viscoplastic model for soft clays." *Int. J. Solids Struct.*, 47(5), 665–677.
Zhang, Z., and Sun, Y. (2011). "Analytical solution for a deep tunnel with arbitrary cross section in a transversely isotropic rock mass." *Int. J. Rock Mech. Min. Sci.*, 48(8), 1359–1363.
Zheng, Y., and Kong, L. (2010). *Geotechnical plastic mechanics*, China Architecture Building Press, Beijing (in Chinese).
Zhu, Q. Z., Shao, J. F., and Mainguy, M. (2010). "A micromechanics-based elastoplastic damage model for granular materials at low confining pressure." *Int J. Plast.*, 26(4), 586–602.